Polymerization-Induced Epitaxy: Scanning Tunneling Microscopy of a Hydrogen-Bonded Sheet of Polyamide on Graphite

Masahito Sano,* Darryl Y. Sasaki, Toyoki Kunitake†

A molecularly thin film of a two-dimensional polymer network formed by hydrogen bonding was synthesized and investigated with scanning tunneling microscopy. Poly(ε-caprolactam) (nylon 6) was epitaxially grown on the basal plane of graphite and an ultrathin film of the polymer was obtained after the bulk materials had been washed away with solvents. The polymer chain has a planar, all-*trans* conformation and adjacent chains run in the antiparallel direction. This produces complete pairing of hydrogen bonding groups, with each amide group lying on a straight line perpendicular to the polymer backbone. This hydrogen-bonded sheet is oriented so that each polymer backbone lies in the (10$\bar{1}$0) direction on the graphite hexagonal lattice, as opposed to the (11$\bar{2}$0) direction taken by other paraffinic molecules studied so far. This experiment shows that hydrogen bonding can be used to control the orientation of macromolecules in two dimensions.

Epitaxially grown films of macromolecules have been produced on a solid surface by conventional synthetic methods (*1*). After such growth, one can obtain ultrathin films by simply washing the surface to remove bulk polymers. The molecular structure can then be directly studied by scanning tunneling microscopy (STM). We have reported that epitaxially grown polyethers on graphite can assume various types of interchain packings as well as a number of epitaxial orientations with respect to the graphite lattice (*1*, *2*). Evidently, the ether oxygen behaves simply as a part of the *trans* zigzag chain, contributing little in the determination of the two-dimensional (2-D) structure of the epitaxial films. However, experiments on poly(ε-caprolactone) on graphite revealed the importance of the dipole-dipole interaction of the carbonyl group in regulating the epitaxial structure (*3*).

We report here on a study of an epitaxial film of poly(ε-caprolactam) (nylon 6). We chose this polyamide not only because of its well-known physical and chemical properties but also to make a comparison with the previous studies. Although structurally similar, epitaxial arrays of nylon 6 and poly(ε-caprolactone) are quite different in that the latter is organized through dipole-dipole interaction and the former is dominated by hydrogen bonding. In this respect, nylon 6 represents an epitaxy of a 2-D sheet rather than that of an array of 1-D, long straight rods.

ε-Caprolactam was polymerized by anionic ring-opening polymerization in dimethoxyethane solution at 135°C with catalytic amounts of sodium hydride and *N*-acetyl-ε-caprolactam (*4*). Freshly cleaved, highly oriented pyrolytic graphite (HOPG) was immersed in the reaction mixture at an early stage of reaction (either before or after the initiation step). The graphite was taken out after the reaction was quenched with ethanol and the surface was cleaned of large adsorbates by washing with hot acetic acid.

The formation of a thin film of nylon 6 on HOPG was confirmed by Fourier transform infrared spectroscopy (FTIR) and x-ray photoelectron spectroscopy (XPS). The FTIR measurements showed peaks at ~2940 and 2850 cm^{-1}, indicating the presence of an aliphatic chain; XPS exhibited substantial increases of oxygen and nitrogen after polymerization, with no sodium present. These observations indicated that only polyamide remained on the HOPG surface after washing.

The STM was operated in air at ambient conditions, and a mechanically cut Pt-Ir wire was used as a tip (*5*). The adsorbate images (Fig. 1) were as easy to obtain as those of the graphite lattice on a bare HOPG surface. These images are not the graphite artifacts, because the underlying graphite could be imaged by bringing the tip closer to the surface. This image is characterized by lines of bright atoms, with less bright atoms in between, forming straight lines 17.2 Å apart. The short distance between the bright spots along the line is 4.3 Å. A similar linear alignment of bright spots was also seen in the case of polyether and polyester.

As in our earlier studies (*1–3*), the following assumptions were made in interpreting the STM images. (i) On bare graphite, alternate carbon atoms contribute strongly to the tunneling current and appear bright. The adsorbate atoms in the vicinity of this brighter graphite carbon atom appear brighter than others that are away from it (*6*). (ii) A polyamide molecule consists of four major types of atomic species other than hydrogen: an aliphatic carbon, a carbonyl carbon, an amide nitrogen, and a carbonyl oxygen. Consistent with the previous studies, the amide nitrogen and the carbonyl group are assigned as the enhanced current sites in a polyamide molecule.

On the basis of these assumptions, a planar zigzag model consistent with the STM image (Fig. 1) is shown in the schematic drawing of Fig. 2, where the carbonyl groups are arbitrarily assumed to be the brightest atoms. Other models can be constructed to give the same STM image by inverting the chain direction or by shifting

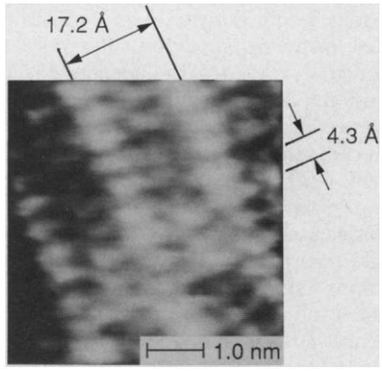

Fig. 1. STM image of nylon 6. No baseline correction was made on any of the images presented.

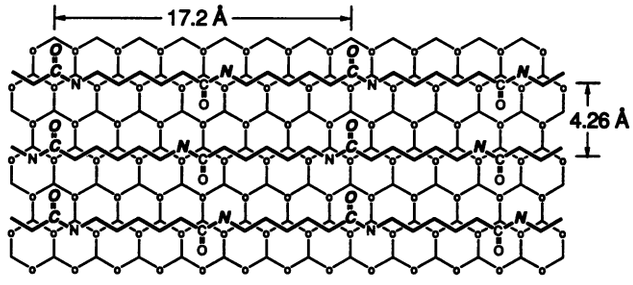

Fig. 2. Schematic drawing showing the epitaxial orientation seen in Fig. 1. A small circle on the graphite hexagonal lattice indicates the brighter carbon atom. The bold characters on a polymer chain represent the atomic species close to the brighter graphite carbon. In this model, the carbonyl groups are assumed to produce the strongest measured current.

Molecular Architecture Project, Research Development Corporation of Japan, Kurume Research Park, Kurume, Fukuoka 830, Japan.

*To whom correspondence should be addressed.
†Permanent address: Department of Chemical Science and Technology, Faculty of Engineering, Kyushu University, Fukuoka 812, Japan.

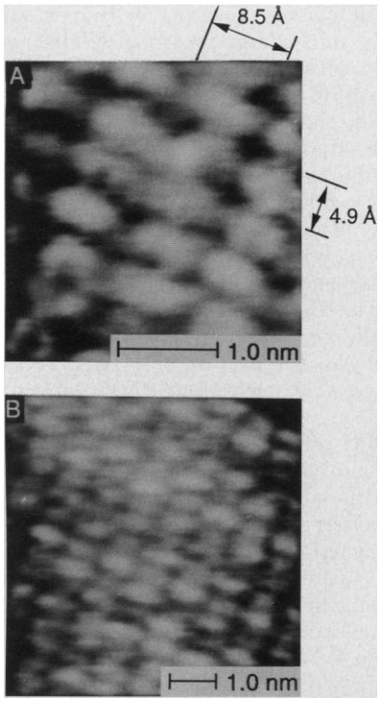

Fig. 3. High-resolution STM image of nylon 6 (**A**) taken at the same location as the image in (**B**). These images are, by far, the most frequently observed.

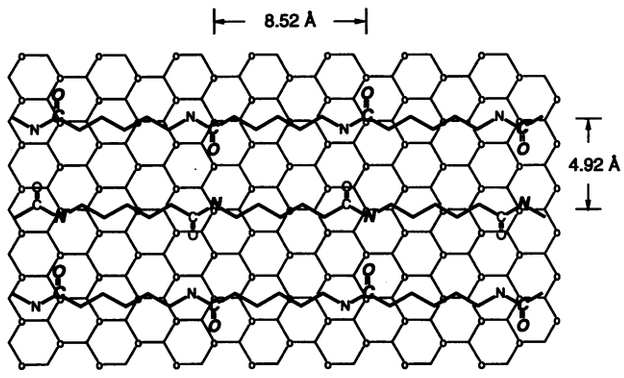

Fig. 4. Schematic drawing representing the images of Fig. 3. The polymer chain lies along the (10$\bar{1}$0) direction, and the hydrogen bonding pairs are on the straight line perpendicular to the polymer backbone.

the adjacent chain by an amount that depends on the relative current intensity of the amide nitrogen and the carbonyl group. In all cases, an all-*trans* conformation requires that every other amide group be the relevant repeating unit. The schematic repeating distance of 17.2 Å (seven graphite hexagonal units) is in complete agreement with the STM image and also with the value taken by the planar zigzag structure of the bulk polymer (*7*, *8*). The polymer backbone lies in the next nearest neighbor direction (11$\bar{2}$0) of the graphite hexagonal lattice (*9*), making the chains 4.26 Å apart. This orientation requires the interchain hydrogen bonding N–H· · ·O=C pairs to lie on a nonstraight line perpendicular to the chain backbone.

The STM image (Fig. 1) correlates well with those of polyether and polyester. However, for nylon 6, this occurred only rarely. Out of over a hundred images observed, more than 90% were characterized by the square arrangement of the rectangular bright regions, separated by 8.5 Å on the long axis and by 4.9 Å on the short axis (Fig. 3). No moiré pattern is visible in the wider scan image of Fig. 3B. A 2-D structure consistent with these images is shown in Fig. 4. The polymer backbone now lies in the nearest carbon neighbor direction (10$\bar{1}$0) of the graphite lattice (*9*). The markedly different appearance of Fig. 3 from that of Fig. 1 is expected from the first assumption made for STM contrast but with a different orientation of the polymer chain with respect to the graphite lattice. This orientation places every amide group on the relevant repeating unit, which is separated by 8.52 Å as measured by the graphite hexagonal unit and with a chain separation of 4.92 Å. This repeating length requires a strain on the polymer backbone relative to the bulk crystalline structure of only 1%. The chain packing is similar to that of nylon 6 on KCl proposed earlier (*10*), although the epitaxial orientation relative to the solid surface is quite different.

The importance of the hydrogen bonding interaction in creating the 2-D array can be inferred if one compares the data presented here with those for poly(ϵ-caprolactone) (*3*). Although the polyester has the same chemical repeating length as nylon 6 and satisfies the lattice matching condition, the polyester chain grows in the (11$\bar{2}$0) direction, whereas the nylon 6 chain lies in the (10$\bar{1}$0) direction. Poly(ϵ-caprolactone) chains pack such that each carbonyl group is placed as far apart as possible (each adjacent chain shifted mutually by two graphite hexagonal units) (*3*). If this polyester grows in the (10$\bar{1}$0) direction assuming the same packing structure, the number of repeating units and the number of chains required in a unit cell of the commensurate structure become necessarily large. As for nylon 6, the hydrogen bonding forces the next amide group to follow on a straight line perpendicular to the polymer backbone, keeping every amide group on a graphite node. Only one monomer unit and one chain are required to form a unit cell for nylon 6.

The fact that in nylon 6 the (10$\bar{1}$0) structure dominates over the (11$\bar{2}$0) structure is interesting, because the (11$\bar{2}$0) structure is the more favorable orientation for the interaction between the aliphatic hydrogen and the graphite hexagonal lattice (*9*, *11*). This latter interaction has been a major factor governing the epitaxial orientations of other polymers (*2*, *3*) and of small molecular crystals (*12*). A recent theoretical calculation of hydrogen bonding among small amide molecules in free space shows weak dependence on the angles of N–H· · ·O and

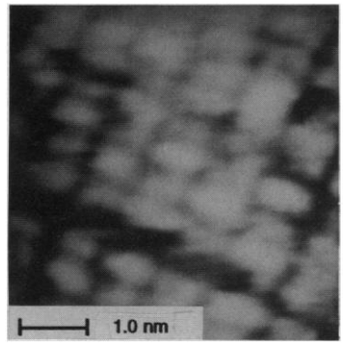

Fig. 5. STM image of nylon 6. This image is basically the same as the ones in Fig. 3 except for the presence of dark bands running along the polymer backbone.

H· · ·O=C (*13*). Thus, an oriented array of hydrogen-bonded pairs over a 2-D network, together with a contribution from the interaction with the graphite hexagonal lattice, needs to be considered to explain the observed stability.

Although the reaction mechanism of polymerization-induced epitaxy is not known, STM can provide some information concerning the chain ordering mechanism. Because the monomer is polymerized by a ring-opening reaction, the chain direction defined by the amide nitrogen attached to the carbonyl group signifies the direction of chain propagation. For instance, the parallel alignment of adjacent chains suggests that each chain is polymerized independently toward the same direction. The alignment in Fig. 4 is antiparallel. This indicates that either a 2-D chain folding or other highly cooperative steps need to be considered. In fact, some images as shown in Fig. 5 are frequently encountered. This image belongs to the same type as illustrated in Fig. 3, but with dark bands running along the polymer backbone in every four to five rows. A possible explanation of this feature is that, as the chain grows by the chain-folding mechanism, it meets the next chain already in position so that the growing chain cannot be further epitaxially po-

lymerized as a result of a steric barrier or an unfavorable lattice matching. In this case, a dark band defines one folding unit.

REFERENCES

1. M. Sano, D. Y. Sasaki, T. Kunitake, *J. Chem. Soc., Chem. Commun.*, in press.
2. M. Sano, D. Y. Sasaki, T. Kunitake, *Macromolecules*, in press.
3. _____, *Proc. Jpn. Acad. B* **68**, 87 (1992).
4. H. K. Hall, Jr., *J. Am. Chem. Soc.* **80**, 6404 (1959).
5. M. Sano and T. Kunitake, *J. Vac. Sci. Technol. B* **9**, 1137 (1991).
6. G. C. McGonigal, R. H. Bernhardt, D. J. Thomson, *Appl. Phys. Lett.* **57**, 28 (1990).
7. D. R. Holmes, C. W. Bunn, D. J. Smith, *J. Polym. Sci.* **17**, 159 (1955).
8. H. Arimoto, M. Ishibashi, M. Hirai, Y. Chatani, *J. Polym. Sci. A* **3**, 317 (1965).
9. P. R. Baukema and A. J. Hopfinger, *J. Polym. Sci. Polym. Phys. Ed.* **20**, 399 (1982).
10. J. Willems, *Experientia* **23**, 409 (1967).
11. A. J. Groszek, *Proc. R. Soc. London Ser. A* **314**, 473 (1970).
12. For liquid crystals, see, for example, D. P. E. Smith, J. K. H. Hörber, G. Binnig, H. Nejoh, *Nature* **344**, 641 (1990).
13. J. J. Novoa and M.-H. Whangbo, *J. Am. Chem. Soc.* **113**, 9017 (1991).

14 May 1992; accepted 20 July 1992

Small-Angle Synchrotron X-ray Scattering Reveals Distinct Shape Changes of the Myosin Head During Hydrolysis of ATP

Katsuzo Wakabayashi, Makio Tokunaga, Izumi Kohno, Yasunobu Sugimoto, Toshiaki Hamanaka, Yasunori Takezawa, Takeyuki Wakabayashi, Yoshiyuki Amemiya

In the energy transduction of muscle contraction, it is important to know the nature and extent of conformational changes of the head portion of the myosin molecules. In the presence of magnesium adenosine triphosphate (MgATP), fairly large conformational changes of the myosin head [subfragment-1 (S1)] in solution were observed by small-angle x-ray scattering with the use of synchrotron radiation as an intense and stable x-ray source. The presence of MgATP reduced the radius of gyration of the molecule by about 3 angstrom units and the maximum chord length by about 10 angstroms, showing that the shape of S1 becomes more compact or round during hydrolysis of MgATP. Comparison with various nucleotide-bound S1 complexes that correspond to the known intermediate states during ATP hydrolysis indicates that the shape of S1 in a key intermediate state, S1-bound adenosine diphosphate (ADP) and phosphate [S1.ADP.P_i], differs significantly from the shape in the other intermediate states of the S1 adenosine triphosphatase cycle as well as that of nucleotide-free S1.**

Conformational changes of the myosin head have been widely investigated because of their possible role in the molecular mechanism of muscle contraction and other myosin-driven motile systems. In vitro motility assays in which the head alone was used strongly suggest that internal motions of the myosin head play an important role in the sliding movement of the actin filaments (*1*). Many physicochemical studies [see, for example, (*2*, *3*)] have indicated that changes of the myosin head occur during hydrolysis of ATP. Such conformational changes have been attributed to the internal flexibility of the head (*3*). Recent electron microscopy (EM) studies, in conjunction with ATP hydrolysis, have revealed the possibility of comparatively large shape changes of the head both for the isolated myosin (*4*) and actin-S1 complexes (*5*, *6*). In contrast, previous x-ray and neutron small-angle scattering studies have not shown a distinct change in the head structure on binding of nucleotide (an ATP analog) (*7*) or on "invisible" F-actin (*8*), suggesting that no significant change occurs in the head during activity.

In this report we present direct evidence for a structural change in the myosin head (S1) during active hydrolysis of MgATP. Improved methods of small-angle x-ray scattering were used with synchrotron radiation as an intense and stable x-ray source. The correlation between changes in the S1 structure and biochemical states thought to be part of the S1 adenosine triphosphatase (ATPase) cycle was determined.

Papain-treated chicken S1 [molecular mass 130 kD (*9*)], which has a full component of the light chains (*10*, *11*), was used immediately after purification by gel filtration, and only peak fractions were retained. A series of x-ray measurements on nucleotide-free and various nucleotide-bound S1 complexes were made with the use of an exposure time of 3 min at 18.5°C (*12*). Protein concentrations were varied from 3 to 7 mg/ml. X-ray measurements on S1 in the presence of 5 mM MgATP were started within 0.5 min after S1 was mixed with ATP. Because the rate constant of MgATP hydrolysis by S1 in solution is ~0.05 s^{-1} at room temperature (*13*), most of the ATP (at least 4 mmol) should remain unhydrolyzed at the end of the x-ray measurement.

Small-angle x-ray scattering curves are presented in Fig. 1 as Guinier plots {ln[$I(S)$] versus S^2 plots} (*14*), where $I(S)$ is the scattered x-ray intensity and $S = 2\sin\theta/\lambda$ (where 2θ is the scattering angle and λ is the x-ray wavelength). The Guinier plots from all S1 samples gave straight lines in the range of $S^2 \leq 0.223 \times 10^{-4}$ Å^{-2} (S^2_{max}), and there was no evidence of upward curvature at lower values of S^2 that would have resulted from aggregation of the molecules in solution (*14*, *15*). The straight region (the Guinier region) was narrow,

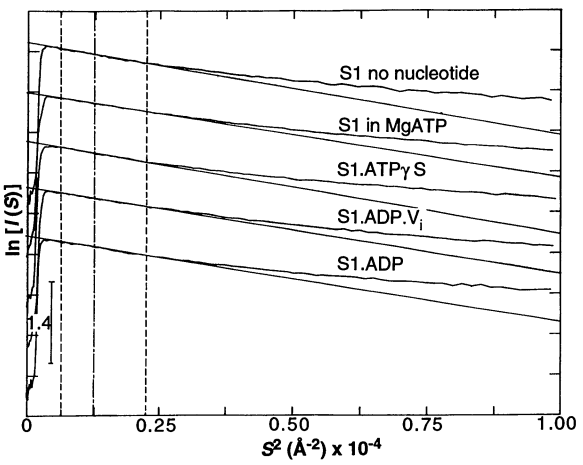

Fig. 1. Typical small-angle x-ray scattering curves of various S1 samples on a Guinier plot. These plots are 7 mg/ml data. The straight lines represent extrapolated Guinier fits. The fitting ranges (the Guinier regions) of the straight lines are indicated by vertical dashed lines [$S^2 = 0.0778 \times 10^{-4}$ Å^{-2} (S^2_{min}) and $S^2 = 0.2228 \times 10^{-4}$ Å^{-2} (S^2_{max})]. The dotted chain line at 0.12×10^{-4} Å^{-2} shows the S^2 value of the present Guinier's criterion (*21*). For clarity, the curves have been shifted successively by 0.8 unit on the ln[$I(S)$] axis.

K. Wakabayashi, I. Kohno, Y. Sugimoto, T. Hamanaka, Y. Takezawa, Department of Biophysical Engineering, Faculty of Engineering Science, Osaka University, Toyonaka, Osaka 560, Japan.
M. Tokunaga and T. Wakabayashi, Department of Physics, Faculty of Science, University of Tokyo, Bunkyo-ku, Tokyo 113, Japan.
Y. Amemiya, the Photon Factory, National Laboratory for High Energy Physics, Tsukuba, Ibaraki 305, Japan.